Proc. NIPR Symp. Upper Atmos. Phys., **9**, 56-62, 1996

INVESTIGATION OF PLASMA DENSITY DISTURBANCES CAUSED BY SPACECRAFT-PLASMA INTERACTIONS AT 4 R_S

Masaki OKADA[1], B.T. TSURUTANI[2], B.E. GOLDSTEIN[2], Hiroshi MATSUMOTO[3], A.L. BRINCA[4] and P.J. KELLOGG[5]

[1]*National Institute of Polar Research, 9-10, Kaga 1-chome, Itabashi-ku, Tokyo 173*
[2]*Jet Propulsion Laboratory, California Institute of Technology, U.S.A.*
[3]*Radio Atmospheric Science Center, Kyoto University, Uji 611*
[4]*Centro de Electrodinamica, Instituto Superior Tecnico, Portugal*
[5]*School of Physics and Astronomy, University of Minnesota, U.S.A.*

Abstract: The proposed Small Solar Probe mission features a close approach to the sun with a perihelion of 4 R_s. Carbon molecules emitted from the spacecraft's heat shield will become ionized by electron impact and photoionization. The newly created ions and electrons may generate electromagnetic and electrostatic plasma waves which are possible sources of interference with *in-situ* plasma measurements. To understand this possible interference, we have performed computer simulations to model the plasma particle distributions caused by the pick-up process of C_2^+ ions and related electrons as the spacecraft flies across the external solar coronal magnetic field. In order to study the wave-particle interactions, which includes inhomogeneities (of the C_2^+ plasma) and kinetic effects, we use the electromagnetic particle code called Kyoto University Electromagnetic Particle Code (KEMPO). We find that there are no substantial density disturbances such as neither shock nor instabilities. The electric field disturbance in the vicinity of the spacecraft is also small enough to detect the solar wind plasma.

1. Model

A full-particle simulation code is used to study inhomogeneities in a solar wind-spacecraft interaction. We use 2-dimensional KEMPO code (MATSUMOTO and OMURA, 1984) to solve for the electromagnetic and electrostatic fields and for particle trajectories. This code solves the full set of Maxwell's equations for the electric and magnetic fields and the equation of motion for the particles in the system. They are solved self-consistently based on the particle-in-cell method (MATSUMOTO *et al.*, 1988; OMURA and MATSUMOTO, 1988). Since the KEMPO code treats both electrons and ions as charged particles, it allows us to investigate nonlinear phenomena due to their kinetic effects.

$$\frac{1}{c^2}\frac{\partial \boldsymbol{E}}{\partial t} = \nabla \times \boldsymbol{B} - \mu_0 \boldsymbol{J}, \tag{1}$$

$$\frac{\partial \boldsymbol{B}}{\partial t} = -\nabla \times E, \tag{2}$$

$$\nabla \cdot \boldsymbol{B} = 0, \tag{3}$$

$$\nabla \cdot \boldsymbol{E} = \frac{\rho}{\varepsilon_0}, \tag{4}$$

$$\frac{d\boldsymbol{v}}{dt} = q(\boldsymbol{E} + \boldsymbol{v} \times \boldsymbol{B}), \tag{5}$$

$$\frac{d\boldsymbol{r}}{dt} = v. \tag{6}$$

Maxwell's equations are solved by a leap-frog scheme for time advancement and a centered differential scheme is used for spatial differentiation. The equations of motion for particles are solved with a Buneman-Boris method (BIRDSALL and LANGDON, 1985). In our simulation model (see Fg. 1), a half open boundary condition is adopted. That is, damping regions are added in both x boundaries and periodic boundary conditions are used in the y direction. The plasma waves propagating in the x direction are damped near the edges of the simulation box (see Fig. 1) and particles are not traced beyond the $x=0$, x_{max} boundary. x_{max} represents the size of the system including the damping regions. At the center of the system we put in an internal boundary which corresponds to the spacecraft. This is indicated by the shaded box of size $2R_0$. In this model all particles impinging upon the spacecraft surface are absorbed, that is, the reflection coefficient of the particles at the spacecraft surface is assumed to be zero. The potential of the spacecraft is calculated from the accumulated charge using a capacitance matrix method (HOCKNEY and EASTWOOD, 1988). The solar wind flows along x axis from left-to-right and the solar wind magnetic field has an angle θ relative to the flow direction and lies within the x-y plane. We choose the spacecraft as our frame of reference. The external electric field has an intensity of $-v_d \times \boldsymbol{B}_0$, where the $\boldsymbol{v}_d = \boldsymbol{v}_{sc} - \boldsymbol{v}_{sw}$. The $\boldsymbol{v}_{sc}$ and $\boldsymbol{v}_{sw}$ are the spacecraft velocity and the solar wind velocity, respectively. This is in the $-z$ direction, *e.g.*, into the paper. In order to simulate an open boundary system, the solar wind particles are injected from both ends (because of the large thermal velocities, some particles enter the box from the right side), $x=0$, x_{max}, with a constant ambient flux which is calculated from the thermal velocity and the solar wind velocity $\boldsymbol{v}_{sw}$.

Table 1 gives the model parameters. We find the electron beta, ion sound Mach number and Alfvén mach number are 0.013, 5.0 and 0.4, respectively. Note that the flow speed is supersonic but not super-Alfvénic. The characteristic frequencies of each species are chosen to maintain realistic ratios relative to the electron cyclotron frequency (AL'PERT,

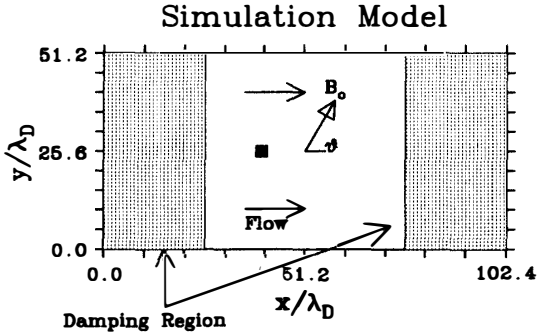

Fig. 1. Simulation model.

Table 1. Normalized parameters used in the computer experiments. Normalizations are taken with respect to the electron cyclotron frequency, Ω_e, the solar wind electron thermal velocity, V_e.

Parameters		
Electron plasma frequency	Π_e/Ω_e	4.0
Proton cyclotron frequency	Ω_P/Ω_e	0.0625
Proton plasma frequency	Π_P/Ω_e	1.0
Proton thermal velocity	V_P/V_e	0.1
C_2^+ cyclotron frequency	Ω_{C2+}/Ω_e	0.01
C_2^+ plasma frequency	Π_{C2+}/Ω_e	0.01
C_2^+ thermal velocity	V_{C2+}/V_e	0.001
Mass ratio	$m_{C2} : m_p : m_e$	100 : 16 : 1
Debye length	λ_D	0.25
Spacecraft size	R_0/λ_D	1.6
Alfvén velocity	V_A/V_e	1.25
Electron beta	β_e	0.013
Plasma drift velocity	V_d/V_e	0.5
Light speed	c/V_e	10
Ion sound speed	V_s/V_e	0.1
Sound mach number	M_s	5.0
Alfvén mach number	M_A	0.4
Spatial grid	Δ_r	0.2
Time grid	Δ_r	0.01
Normalization values		
Electron cyclotron frequency	Ω_e	1.0
Solar wind electron thermal velocity	V_e	1.0

1990; BRINCA and TSURUTANI, 1989). The drift, ion thermal and ion sound velocities are indicated with a value normalized to the solar wind electron thermal velocity. Solar wind electrons and ions are considered to be isothermal. The mass ratios of the electrons, protons and C_2 ions are assumed to be 1 : 16 : 100 in our simulation. The compressed mass ratio is necessary for reasons of computational efficiency. The thermal velocity of C_2-origin electrons is assumed to be 10 times smaller than that of solar wind electrons. The thermal velocity of C_2 ions is very small, and therefore the ions can be assumed to be a cold beam in the solar wind. Figure 2 shows the velocity distribution function used in the computer simulations.

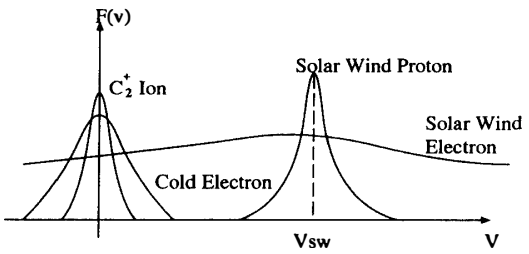

Fig. 2 Velocity distribution function used in the computer experiments.

Carbon molecules are emitted from the spacecraft's heat shield will become ionized by electron impact and photoionization. We estimate the neutral C_2 density, ρ_{c_2}, as a function of distance from the spacecraft, r. The neutral C_2 particles flow isotropically outward from the spacecraft. The density as a function of r is:

$$\rho_{c_2}=\frac{Q}{4M_{c_2}\pi r^2 V_n}, \tag{7}$$

wherm Q is mass loss rate of the carbon heat shield in gs^{-1}, M_{c2} is mass of C_2 ions in g, r is the distance fsom the spacecraft in cm, and V_n is the outflow velocity of neutrals in cm s^{-1}. The ionization time of C_2 particles at 4 R_s is assumed to be $\tau=1.7\times10^{-2}$ s^{-1} (GOLDSTEIN *et al.*, 1980). Assuming a spacecraft radius of 2 m, an upper limit for the C_2^+ density is estimated assuming no removal by solar wind electric field (*i.e.,* out flow of newly created ions with their initial velocity V_n):

$$\rho_{C_2+}(r_0)=\frac{\int_{200}^{r_0} r^2\rho_{C_2}\tau dr}{r_0^2 V_n}. \tag{8}$$

An upper limit for Q is 2.5×10^{-3} g s^{-1} and $V_n=1.0\times10^5$ cm s^{-1}. We assume that the C_2^+ ions are injected in the simulation box with the spatial profile shown in eq. (8). The maximum pickup ion density is about 1.3×10^4 cm^{-3} at a distance of 4×10^2 cm from the spacecraft surface.

2. Results

We perform 4 computer simulation runs with different values of the angle of the external magnetic field relative to the solar wind flow direction and C_2 densities. Parameters for each simulation run are listed in Table 2. We first performed a computer simulation without C_2 particles ($\theta=30°$) to understand the effect of the C_2^+ emission. We did this for baseline information and confirmed that only the solar wind proton forms a small wake. Next we put the C_2 pickup plasma into the system and compare the difference between two cases at four different θ values ($\theta=0°, 30°, 60°$ and $90°$). The larmor radius is 200 λ_D, larger than the simulation box, 51.2 λ_D.

The 4 figures (Figs. 3, 4, 5 and 6) illustrate the densities when C_2 ions are present. Figure 3 is the case where the external magnetic field has an angle of 0° relative to the solar wind flow direction. The density profiles of C_2-origin electrons (a) and C_2^+ ions (b) are shown, respectively. A solar wind ion wake is formed behind the spacecraft while the

Table 2. Parameters used in the simulation runs. C_2 number flux is defined relative to the solar wind particle number flux.

Case No.	Fig. No.	$\theta°$	Relative C_2 flux
(1)	3	0.0	0.5
(2)	4	30.0	0.5
(3)	5	60.0	0.5
(3)	6, 7	90.0	0.5

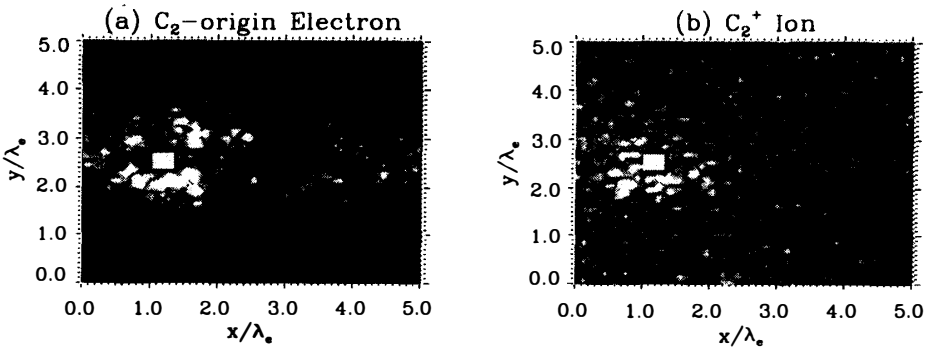

Fig. 3. Plasma particle number density contour in the case where $\theta = 0°$.

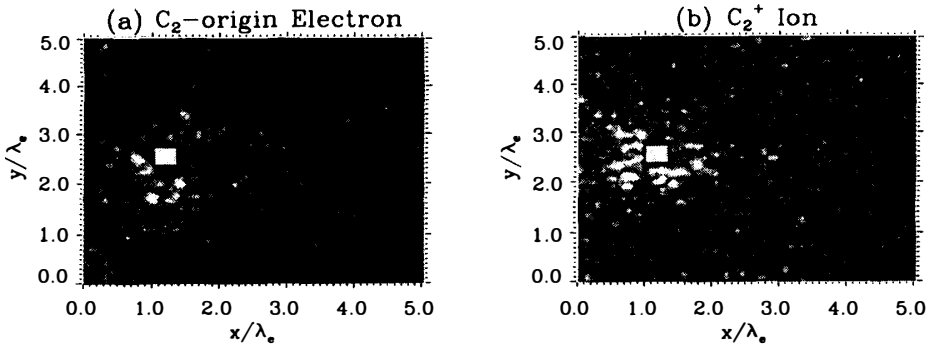

Fig. 4. Same as Fig. 3 but for $\theta = 30°$.

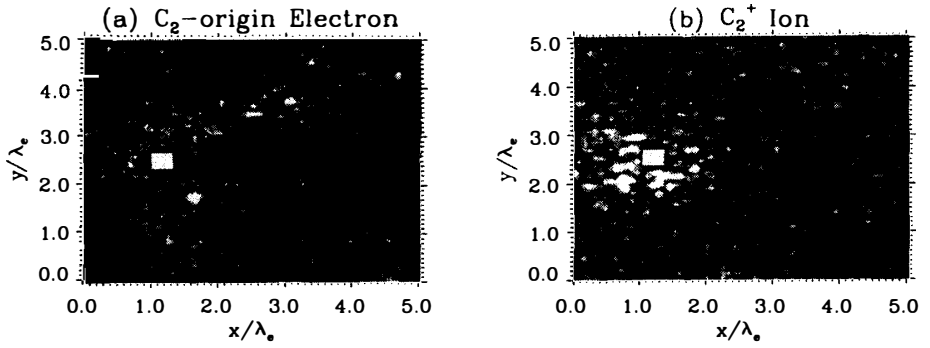

Fig. 5. Same as Fig. 3 but for $\theta = 60°$.

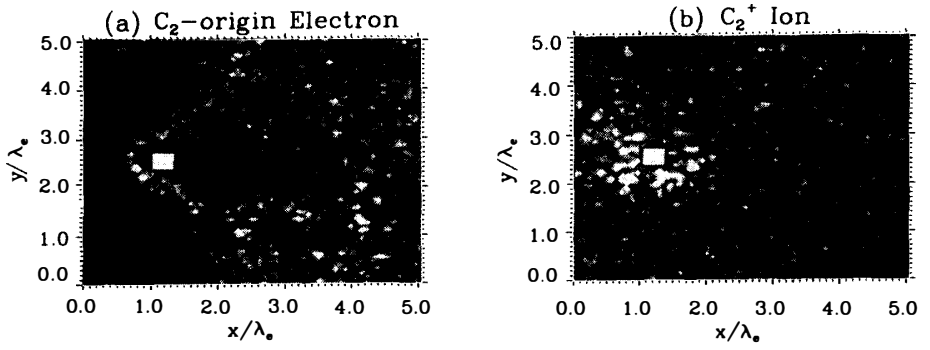

Fig. 6. Same as Fig. 3 but for $\theta = 90°$.

solar wind ion wake is very small without the C_2^+ ions case (not shown). This is primarily caused by the C_2 ion density enhancement near the spacecraft (shown in panel (b)), displacing the solar wind protons. There is a C_2 ion density buildup in the vicinity of the spacecraft (panel (b)). The largest densities are on the upstream side of the spacecraft. While the newly created C_2^+ ions are removed slowly from the vicinity of the spacecraft, the C_2-origin electrons are carried away very fast by interacting with the solar wind electrons.

As the angle of the magnetic field relative to the spacecraft velocity increases (Figs. 4 to 6), more C_2 electrons are carried away from the spacecraft. The C_2 ions again build up on the upstream side of the spacecraft. For the $\theta=30^\circ$ and 60° cases, the absolute densities are almost the same as the $\theta=0^\circ$ case, but the C_2^+ ion density structure is now much broader in angle. Note the $\boldsymbol{E}\times\boldsymbol{B}$ flow direction is from the upper left to lower right and therefore the asymmetry in the C_2 electrons in the y direction. This density asymmetri is clearly seen in eq. (5).

Figure 6 represents the solar wind and C_2 plasma density with the same format as the previous figure but for $\theta=90^\circ$. Because of the orthogonal field orientation, the C_2 electron density enhancement in the upstream region is now symmetric about the y direction.

Figure 7 depicts the potential structure around the spacecraft with a bird's eye view for the $\theta=90^\circ$ case. A potential hill due to charge separation between C_2 electrons and ions can be send in downstream region of the spacecraft. The potential of the spacecraft itself is not affected much by spacecraft charging effects. The potential of the spacecraft is almost -2.6×10^{-2} of the electron thermal energy ($\varkappa_B T_e$). Comparing with no C_2 emission case, we confirmed that the spacecraft potential is not affected by the C_2 emission (TSURUTANI, 1991). The corresponding electric field at the spacecraft surface over the Debye length is $\sim5.2\times10^{-2}$ Vm^{-1}. Two orders of magnitude lower than the $v_d\times\boldsymbol{B}_0$

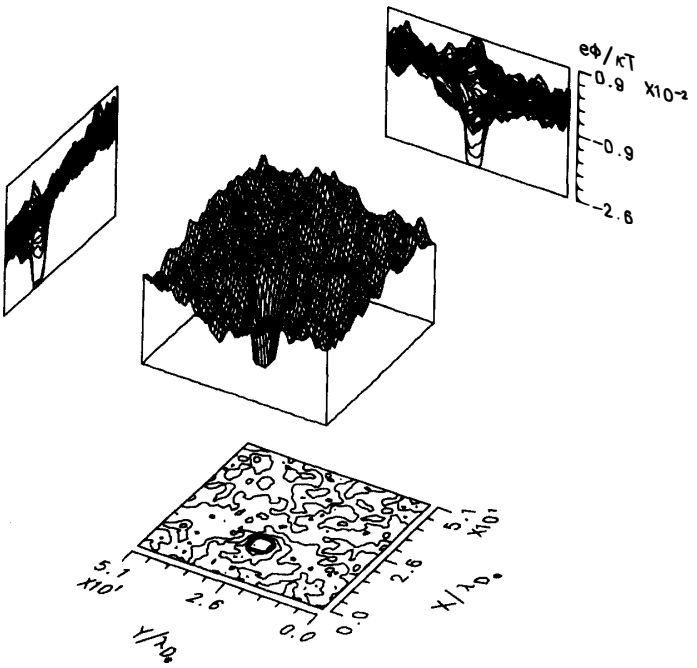

Fig. 7. Potential structure around the spacecraft.

electric field. The maximum of this potential is $\sim -2.6\times 10^{-2}\ \kappa_B T_e \sim 5.0$ eV. The drift energy of the solar wind proton is ~ 100 eV. Thus, this should not lead to any interference with solar wind plasma detection.

3. Summary

We have performed 5 computer simulations, one without C_2 ions and others with C_2 ions and $\theta = 0°, 30°, 60°$ and $90°$. The four cases of the results have been shown in this paper. There is an upstream C_2^+ density feature for all cases of θ. The density enhancement has a magnitude of $\sim 4\ n_0$. The C_2 electron density is affected by the angle θ. Two major C_2 electron density enhancement were observed downstream of the spacecraft. One is due to the $v_d \times \boldsymbol{B}$ drift, and the other is due to the magnetic field aligned flow. There is a measurable electric field disturbance at the surface of the spacecraft but quite small $\sim 5.2\times 10^{-2}$ Vm^{-1} relative to the solar wind drift energy. We confirmed that the solar wind flow is not greatly affected by the potential disturbances in the vicinity of the spacecraft.

References

AL'PERT, Y.L. (1990): Space Plasma, Vol. 2. Cambridge, Cambridge Univ. Press, 19-74.

BIRDSALL, C.K. and LANGDON, A.B. (1985): Plasma Physics *via* Computer Simulation. New York, MacGraw-Hill, 58-63.

BRINCA, A.L. and TSURUTANI, B.T. (1989): Influence of multiple ion species on low-frequency electromagnetic wave instabilities. J. Geophys. Res., **94**, 13565-13569.

GOLDSTEIN, B.E., FELDMAN, W.C., GARRETT, H.B., KATZ, I., LINSON, L., OGILVIE, K.W., SCARF, F.L. and WHIPPLE, E.C. (1980): Spacecraft mass loss and electric potential requirements for the star-probe mission. Jet Propulsion Laboratory, **715-100**.

HOCKNEY, R.W. and EASTWOOD, J.W. (1988): Computer Simulation Using Particles. New York, MacGraw-Hill, 215-219.

MATSUMOTO, H., INAGAKI, K. and OMURA, Y. (1988): Computer simulation of passage of an electron beam through a plasma. Adv. Space. Res., **8**, 151-160.

MATSUMOTO, H. and OMURA, Y. (1984): Particle simulation of electromagnetic waves and its application to space plasmas. Computer Simulation of Space Plasmas, ed. by H. MATSUMOTO and T. SATO. Tokyo, Terra Sci. Publ., 43-102.

OMURA, Y. and MATSUMOTO, H. (1988): Computer experiments on whistler and plasma wave emission for space lab-2 electron beam. Geophys. Res. Lett., **15**, 319-322.

TSURUTANI, B.T. (1991): COMETS: A Laboratory for Plasma Waves and Instabilities. Washington, D. C., Am. Geophys. Union, 189 p. (Geophysical Monograph 61).

(Received September 4, 1995; Revised manuscript accepted September 25, 1995)